Planning Walking Patterns for a Biped Robot

Qiang Huang, *Member, IEEE*, Kazuhito Yokoi, *Member, IEEE*, Shuuji Kajita, *Member, IEEE*, Kenji Kaneko, Hirohiko Arai, *Member, IEEE*, Noriho Koyachi, *Member, IEEE*, and Kazuo Tanie, *Member, IEEE*

***Abstract*—Biped robots have better mobility than conventional wheeled robots, but they tend to tip over easily. To be able to walk stably in various environments, such as on rough terrain, up and down slopes, or in regions containing obstacles, it is necessary for the robot to adapt to the ground conditions with a foot motion, and maintain its stability with a torso motion. When the ground conditions and stability constraint are satisfied, it is desirable to select a walking pattern that requires small torque and velocity of the joint actuators. In this paper, we first formulate the constraints of the foot motion parameters. By varying the values of the constraint parameters, we can produce different types of foot motion to adapt to ground conditions. We then propose a method for formulating the problem of the smooth hip motion with the largest stability margin using only two parameters, and derive the hip trajectory by iterative computation. Finally, the correlation between the actuator specifications and the walking patterns is described through simulation studies, and the effectiveness of the proposed methods is confirmed by simulation examples and experimental results.**

***Index Terms*—Actuator specification, biped robot, stability, uneven ground, walking pattern generation.**

I. Introduction

BIPED robots have higher mobility than conventional wheeled robots, especially when moving on rough terrain, steep stairs, and in environments with obstacles. Many related issues such as stability criterion [1], [2], actual robot design and application [3]–[7], and dynamics analysis [8]–[12] have been studied.

A focus of many studies has been walking pattern synthesis. Zerrugh *et al.* [13] have investigated the walking pattern for a biped robot by recording human kinematic data. McGeer [14] described a natural walking pattern generated by the passive interaction of gravity and inertia on a downhill slope. To extend the minimum-energy walking method to level ground and uphill slopes, Channon *et al.* [15], Rostami *et al.* [16], and Roussel *et al.* [17] have proposed methods of gait generation by minimizing the cost function of energy consumption. Silva *et al.* [18] have investigated the required actuator power and energy by adjusting walking parameters.

Manuscript received June 12, 2000; revised December 17, 2000. This paper was recommended for publication by Associate Editor I. Walker and Editor A. De Luca upon evaluation of the reviewers' comments. This work was supported by the Humanoid Robotics Project in NEDO Industrial Science and Technology Frontier Program. This paper was presented in part at the IEEE International Conference on Robotics and Automation, Detroit, MI, May 1999.

Q. Huang is with the Department of Mechatronics, Beijing Institute of Technology, Beijing, China 100081 (e-mail: qhuang@bit.edu.cn).

K. Yokoi, S. Kajita, K. Kaneko, H. Arai, N. Koyachi, and K. Tanie are with the Intelligent Systems Institute, National Institute of Advanced Industrial Science and Technology, Ibaraki 305-8568, Japan (e-mail: yokoi@mel.go.jp; kajita@mel.go.jp; kaneko@mel.go.jp; harai@mel.go.jp; koyachi@mel.go.jp; tanie@mel.go.jp).

Publisher Item Identifier S 1042-296X(01)06728-3.

Since a biped robot tends to tip over easily, it is necessary to take stability into account when determining a walking pattern. Zheng *et al.* [20] have proposed a method of gait synthesis for static stability. Chevallereau *et al.* [21] have discussed dynamic stability when specifying a low energy reference trajectory. Unfortunately, this low-energy reference trajectory does not necessarily satisfy the stability constraint.

To ensure the dynamic stability of a biped robot, Takanishi *et al.* [22], Shih *et al.* [23], Hirai *et al.* [24], and Dasgupta *et al.* [25] have proposed methods of walking pattern synthesis based on zero moment point (ZMP) [1]. The ZMP is defined as the point on the ground about which the sum of all the moments of the active forces equals zero. If the ZMP is within the convex hull of all contact points between the feet and the ground, the biped robot is possible to walk. Hereafter, this convex hull of all contact points is called the stable region (see Appendix A). Basically, these investigations first design a desired ZMP trajectory, then derive the hip motion or torso motion required to achieve that ZMP trajectory. The advantage of this method is that the stability margin (see Appendix A) can be large if the desired ZMP is designed near the center of the stable region. However, since the change of the ZMP due to hip motion is limited, not all desired ZMP trajectories can be achieved [28]. Furthermore, to achieve a desired ZMP trajectory, the hip acceleration may need to be large. In this case, since the torso is relatively massive, energy consumption increases, and control for task execution of the upper limbs becomes difficult. Therefore, it is desirable to obtain hip motion without first designing the desired ZMP trajectory.

For a biped robot to be able to walk in various ground conditions, such as on level ground, over rough terrain, and in obstacle-filled environments, the robot must be capable of various types of foot motion. For example, a biped robot should be able to lift its feet high enough to negotiate obstacles, or have support feet with suitable angles to match the roughness of the terrain. Most previous literature has described foot trajectories generated by polynomial interpolation. When there are various constraints such as ground conditions and various foot motions, the order of the polynomial is too high and its computation is difficult, and the trajectory may oscillate. To avoid this problem, Shih [29], [30] presented a method for producing foot trajectories by cubic spline interpolation. Unfortunately, Shih only discussed the implementation of simple boundary constraints and a constant foot angle.

The actuator's size and weight are restricted in developing a human-size biped robot or humanoid robot. Therefore, the power of actuators, the pick-torque, and pick-velocity of joints are limited. When the stability constraint and the ground conditions are satisfied, it is additionally desirable to select a walking

pattern that requires small torque and velocity of the joint actuators. To reach this goal, it is necessary to clarify the relationship between the actuator specifications and the walking patterns. This relationship is also important to select suitable actuators and speed reduction devices such as gears and pulley-belts when designing the actual biped robot. However, this issue has not been sufficiently discussed before.

This paper describes a proposed method for planning walking patterns, which includes the ground conditions, dynamic stability constraint, and relationship between walking patterns and actuator specifications. The paper is organized as follows. The walking cycle of the biped robot is described in Section II. In Section III, we formulate the constraints of a complete foot trajectory and generate the foot trajectory by third spline interpolation. In Section IV, we formulate the problem of smooth hip motion with the largest stability margin using two parameters, and derive the hip trajectory by iterative computation without first designing a desired ZMP trajectory. The correlation between the actuator specifications and walking patterns is discussed with simulation results, and experimental results are provided in Section V. Finally, our conclusions are given in Section VI.

II. Walking Cycle

We considered an anthropomorphic biped robot with a trunk. Each leg consists of a thigh, a shin, and a foot, and has six degrees of freedom (DOF): three DOF in the hip joint, one in the knee joint, and two in the ankle joint.

Biped walking is a periodic phenomenon. A complete walking cycle is composed of two phases: a double-support phase and a single-support phase. During the double-support phase, both feet are in contact with the ground. This phase begins with the heel of the forward foot touching the ground, and ends with the toe of the rear foot leaving the ground. During the single-support phase, while one foot is stationary on the ground, the other foot swings from the rear to the front.

Many studies on gait planning [14]–[18] have assumed that the double-support phase is instantaneous. But in such a case, the related hip has to move too fast. In order to maintain its stability, the robot's center of gravity, in the case of static stability or the ZMP in the case of dynamic stability, must be transferred from the rear foot to the front foot during the short double-support phase. On the other hand, if the interval of the double-support phase is too long, it is difficult for the biped robot to walk at high speed. The interval of the double-support phase in human locomotion is about 20% [33], [34], so we used this value as the basis for our calculation.

If both foot trajectories and the hip trajectory are known, all joint trajectories of the biped robot will be determined by kinematic constraints. The walking pattern can therefore be denoted uniquely by both foot trajectories and the hip trajectory. When the robot moves straightforward, the lateral positions of both feet are constant. The lateral hip motion can be obtained similarly as the sagittal hip motion as discussed in Section IV. In the following sections, we only discuss trajectories in the sagittal plane.

For a sagittal plane, each foot trajectory can be denoted by a vector $\mathbf{X}_{\mathrm{a}} = [x_{\mathrm{a}}(t), z_{\mathrm{a}}(t), \theta_{\mathrm{a}}(t)]^{\mathrm{T}}$, where $(x_{\mathrm{a}}(t), z_{\mathrm{a}}(t))$ is the coordinate of the ankle position, and $\theta_{\mathrm{a}}(t)$ denotes the angle of the foot. The hip trajectory can be denoted by a vector $\mathbf{X}_{\mathrm{h}} = [x_{\mathrm{h}}(t), z_{\mathrm{h}}(t), \theta_{\mathrm{h}}(t)]^{\mathrm{T}}$, where $(x_{\mathrm{h}}(t), z_{\mathrm{h}}(t))$ denotes the coordinate of the hip position and $\theta_{\mathrm{h}}(t)$ denotes the angle of the hip (Fig. 1).

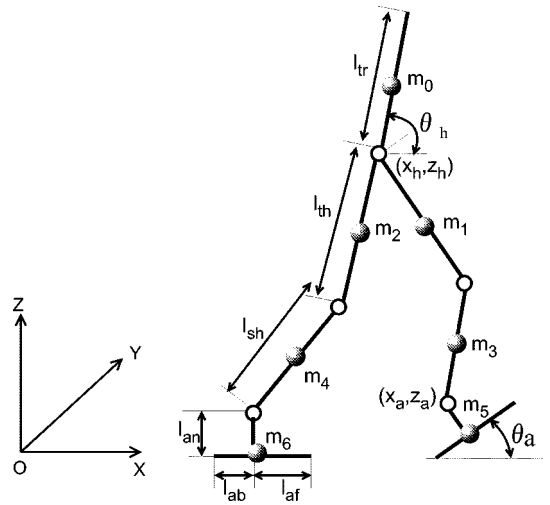

Fig. 1. Model of the biped robot.

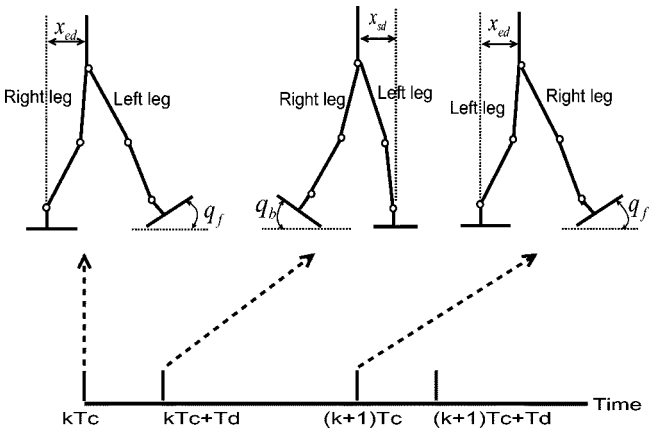

Fig. 2. Walking cycle.

To enable the robot to adapt to various ground conditions, we must first specify both foot trajectories, and then determine the hip trajectory.

III. Foot Trajectories

Assuming that the period necessary for one walking step is T_{c}, the time of the kth step is from kT_{c} to $(k+1)T_{\mathrm{c}}$, $k = 1, 2, \ldots, K$, K is the number of steps. To simplify our analysis, we define the kth walking step to begin with the heel of the right foot leaving the ground at $t = kT_{\mathrm{c}}$, and to end with the heel of the right foot making first contact with the ground at $t = (k+1)T_{\mathrm{c}}$ (Fig. 2). In the following, we discuss only the generation of the right foot trajectory. The left foot trajectory is same as the right foot trajectory except for a T_{c} delay.

Most previous studies have defined foot trajectories in which the feet are always level with the ground, that is, the foot angle $\theta_{\mathrm{a}}(t)$ is always zero. Since the robot cannot touch the ground first by the heel of the forward foot and leave the ground finally

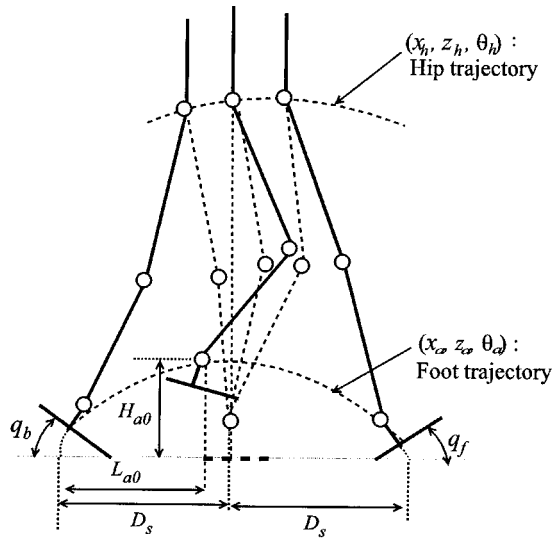

Fig. 3. Walking parameters.

by the toe of the rear foot, these kinds of foot trajectories are not useful for high-speed walking. Additionally, from the viewpoint of natural human locomotion and aesthetics, it is undesirable that the foot slope always be level.

Letting $q_{\rm b}$ and $q_{\rm f}$ be the designated angles of the right foot as it leaves and lands on the ground (Fig. 2), respectively. Assuming that the entire sole surface of the right foot is in contact with the ground at $t = kT_{\rm c}$ and $t = (k+1)T_{\rm c} + T_{\rm d}$, we get the following constraints:

$$\theta_{\rm a}(t) = \begin{cases} q_{\rm gs}(k), & t = kT_{\rm c} \\ q_{\rm b}, & t = kT_{\rm c} + T_{\rm d} \\ -q_{\rm f}, & t = (k+1)T_{\rm c} \\ -q_{\rm ge}(k), & t = (k+1)T_{\rm c} + T_{\rm d} \end{cases} \tag{1}$$

where $T_{\rm d}$ is the interval of the double-support phase, $q_{\rm gs}(k)$ and $q_{\rm ge}(k)$ are the angles of the ground surface under the support foot, particularly $q_{\rm gs}(k) = q_{\rm ge}(k) = 0$ on level ground.

Over rough terrain or in environments with obstacles, it is necessary to lift the swing foot high enough to negotiate obstacles. Letting $(L_{\rm ao}, H_{\rm ao})$ be the position of the highest point of the swing foot (Fig. 3), from (1) and the kinematic constraints, the following constraints must be satisfied. See (2) and (3), shown at the bottom of the page, where $D_{\rm s}$ is the length of one step, $kT_{\rm c} + T_{\rm m}$ is the time when the right foot is at its highest point, $l_{\rm an}$ is the height of the foot, $l_{\rm af}$ is the length from the ankle joint to the toe, $l_{\rm ab}$ is the length from the ankle joint to the heel (Fig. 1), $h_{\rm gs}(k)$ and $h_{\rm ge}(k)$ are the heights of the ground surface which is under the support foot, particularly $h_{\rm gs}(k) = h_{\rm ge}(k) = 0$ on level ground.

Since the entire sole surface of the right foot is in contact with the ground at $t = kT_{\rm c}$ and $t = (k+1)T_{\rm c} + T_{\rm d}$, the following derivative constraints must be satisfied:

$$\begin{cases} \dot{\theta}_{\rm a}(kT_{\rm c}) = 0 \\ \dot{\theta}_{\rm a}((k+1)T_{\rm c} + T_{\rm d}) = 0 \end{cases} \tag{4}$$

$$\begin{cases} \dot{x}_{\rm a}(kT_{\rm c}) = 0 \\ \dot{x}_{\rm a}((k+1)T_{\rm c} + T_{\rm d}) = 0 \end{cases} \tag{5}$$

$$\begin{cases} \dot{z}_{\rm a}(kT_{\rm c}) = 0 \\ \dot{z}_{\rm a}((k+1)T_{\rm c} + T_{\rm d}) = 0. \end{cases} \tag{6}$$

To generate a smooth trajectory, it is necessary that the first derivative (velocity) terms $\dot{x}_{\rm a}(t)$, $\dot{z}_{\rm a}(t)$, and $\dot{\theta}_{\rm a}(t)$ be differential, the second derivative (acceleration) terms $\ddot{x}_{\rm a}(t)$, $\ddot{z}_{\rm a}(t)$, and $\ddot{\theta}_{\rm a}(t)$ be continuous at all t, including all breakpoints $t = kT_{\rm c}$, $kT_{\rm c} + T_{\rm d}$, $kT_{\rm c} + T_{\rm m}$, $(k+1)T_{\rm c}$, $(k+1)T_{\rm c} + T_{\rm d}$.

To satisfy constraint (1)–(6), and the continuity conditions of the first derivative and the second derivative, the order of the polynomial will be too high and its computation is difficult using polynomial interpolation. Therefore, we obtain the foot trajectory by third-order spline interpolation (see Appendix B). In this case, $x_{\rm a}(t)$, $z_{\rm a}(t)$, and $\theta_{\rm a}(t)$ are characterized by third-order polynomial expressions, and the second derivatives $\ddot{x}_{\rm a}(t)$, $\ddot{z}_{\rm a}(t)$, and $\ddot{\theta}_{\rm a}(t)$ are always continuous. By varying the values of constraint parameters $q_{\rm gs}(k)$, $q_{\rm ge}(k)$, $h_{\rm gs}(k)$, $h_{\rm ge}(k)$, $q_{\rm b}$, $q_{\rm f}$, $H_{\rm ao}$, and $L_{\rm ao}$, we can easily produce different foot trajectories.

IV. Hip Trajectory

From the viewpoint of stability, it is desirable that hip motion parameter $\theta_{\rm h}(t)$ is constant when there is no waist joint; in particular, $\theta_{\rm h}(t) = 0.5\ \pi$ rad on level ground. Hip motion $z_{\rm h}(t)$ hardly affects the position of the ZMP. We can specify $z_{\rm h}(t)$ to be constant, or to vary within a fixed range. Assuming that the hip is at its highest position $H_{\rm hmax}$ at the middle of the single-support phase, and at its lowest position $H_{\rm hmin}$ at the

$$x_{\rm a}(t) = \begin{cases} kD_{\rm s}, & t = kT_{\rm c} \\ kD_{\rm s} + l_{\rm an}\sin q_{\rm b} + l_{\rm af}(1 - \cos q_{\rm b}), & t = kT_{\rm c} + T_{\rm d} \\ kD_{\rm s} + L_{\rm ao}, & t = kT_{\rm c} + T_{\rm m} \\ (k+2)D_{\rm s} - l_{\rm an}\sin q_{\rm f} - l_{\rm ab}(1 - \cos q_{\rm f}), & t = (k+1)T_{\rm c} \\ (k+2)D_{\rm s}, & t = (k+1)T_{\rm c} + T_{\rm d} \end{cases} \tag{2}$$

$$z_{\rm a}(t) = \begin{cases} h_{\rm gs}(k) + l_{\rm an}, & t = kT_{\rm c} \\ h_{\rm gs}(k) + l_{\rm af}\sin q_{\rm b} + l_{\rm an}\cos q_{\rm b}, & t = kT_{\rm c} + T_{\rm d} \\ H_{\rm ao}, & t = kT_{\rm c} + T_{\rm m} \\ h_{\rm ge}(k) + l_{\rm ab}\sin q_{\rm f} + l_{\rm an}\cos q_{\rm f}, & t = (k+1)T_{\rm c} \\ h_{\rm ge}(k) + l_{\rm an}, & t = (k+1)T_{\rm c} + T_{\rm d} \end{cases} \tag{3}$$

middle of the double-support phase during one walking step, $z_{\rm h}(t)$ has the following constraints:

$$z_{\rm h}(t) = \begin{cases} H_{\rm hmin}, & t = kT_{\rm c} + 0.5T_{\rm d} \\ H_{\rm hmax}, & t = kT_{\rm c} + 0.5(T_{\rm c} - T_{\rm d}) \\ H_{\rm hmin}, & t = (k+1)T_{\rm c} + 0.5T_{\rm d}. \end{cases} \quad (7)$$

The trajectory of $z_{\rm h}(t)$ that satisfies (7) and the second derivative continuity condition also can be obtained by third spline interpolation.

The change of $x_{\rm h}(t)$ is the main factor that affects the stability of a biped robot walking in a sagittal plane. As analyzed in Section I, some researchers [22]–[25] have presented methods for deriving the hip trajectory to execute a desired ZMP. The defects of these methods are that not all desired ZMP trajectories can be attained and the hip acceleration may need to be very large. To solve these problems, we propose a method consisting of the following steps:

1) generate a series of smooth $x_{\rm h}(t)$;
2) determine the final $x_{\rm h}(t)$ with a large stability margin.

A complete walking process is composed of three phases: a starting phase in which the walking speed varies from zero to a desired constant velocity, a steady phase with a desired constant velocity, and an ending phase in which the walking speed varies from a desired constant velocity to zero. First, the hip motion $x_{\rm h}(t)$ of the steady phase is obtained with the following procedure.

During a one-step cycle, $x_{\rm h}(t)$ can be described by two functions: one for the double-support phase and one for the single-support phase. Letting $x_{\rm sd}$ and $x_{\rm ed}$ denote distances along the x-axis from the hip to the ankle of the support foot at the start and end of the single-support phase, respectively (Fig. 2), we get the following equation:

$$x_{\rm h}(t) = \begin{cases} kD_{\rm s} + x_{\rm ed}, & t = kT_{\rm c} \\ (k+1)D_{\rm s} - x_{\rm sd}, & t = kT_{\rm c} + T_{\rm d} \\ (k+1)D_{\rm s} + x_{\rm ed}, & t = (k+1)T_{\rm c}. \end{cases} \quad (8)$$

To obtain a smooth periodic $x_{\rm h}(t)$ of the steady phase, the following derivative constraints must be satisfied:

$$\begin{cases} \dot{x}_{\rm h}(kT_{\rm c}) = \dot{x}_{\rm h}(kT_{\rm c} + T_{\rm c}) \\ \ddot{x}_{\rm h}(kT_{\rm c}) = \ddot{x}_{\rm h}(kT_{\rm c} + T_{\rm c}). \end{cases} \quad (9)$$

Using third-order periodic spline interpolation [35], we obtain $x_{\rm h}(t)$ which satisfies constraints (8) and (9), and the second derivative continuity conditions is given in (10), shown at the bottom of the next page.

By defining different values for $x_{\rm sd}$ and $x_{\rm ed}$, we get a series of smooth $x_{\rm h}(t)$ according to (10). We specify $x_{\rm sd}$ and $x_{\rm ed}$ to vary within a fixed range, in particular

$$\begin{cases} 0.0 < x_{\rm sd} < 0.5D_{\rm s} \\ 0.0 < x_{\rm ed} 0.5D_{\rm s}. \end{cases} \quad (11)$$

Based on (10) and (11) and the ZMP (13) and (14) (see Appendix A), a smooth trajectory $x_{\rm h}(t)$ with the largest stability margin can be formulated as follows:

$$\max_{x_{\rm ed} \in (0, 0.5D_{\rm s}), x_{\rm sd} \in (0, 0.5D_{\rm s})} d_{\rm zmp}(x_{\rm sd}, x_{\rm ed}) \quad (12)$$

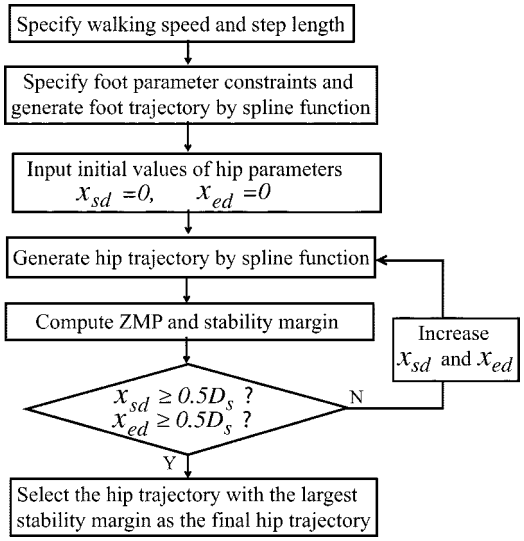

Fig. 4. Algorithm for planning walking patterns.

TABLE I
PARAMETERS OF THE BIPED ROBOT

Length (cm)	l_{tr}	l_{th}	l_{sh}	l_{an}	l_{ab}	l_{af}	
	50	30	30	10	10	13	
Weight (kg)	m_0	m_1	m_2	m_3	m_4	m_5	m_6
	43.0	10.0	10.0	5.7	5.7	3.3	3.3
Inetia (kgm^2)	I_{0y}	I_{1y}	I_{2y}	I_{3y}	I_{4y}	I_{5y}	I_{6y}
	1.69	0.02	0.02	0.08	0.08	0.01	0.01

where $d_{\rm zmp}(x_{\rm sd}, x_{\rm ed})$ denotes the stability margin. Since there are only two parameters $x_{\rm sd}$ and $x_{\rm ed}$, we can easily obtain solutions for (12) by exhaustive search computation (Fig. 4).

Determining $x_{\rm h}(t)$ of the steady phase also specifies the final constraints of the starting phase and the initial constraints of the ending phase. The initial constraints of the starting phase, such as $\dot{x}_{\rm h}(t_0) = 0$, and the final constraints of the ending phase, such as $\dot{x}_{\rm h}(t_e) = 0$, are known. Therefore, $x_{\rm h}(t)$ of the starting phase and ending phase can be obtained by third-order spline interpolation.

V. SIMULATION AND EXPERIMENT

To compute the required actuator specifications such as torque and velocity, it is necessary to accurately formulate and solve the equations of the kinematics and dynamics of the robot mechanisms. To solve this problem, we have developed a dynamic simulator [31] based on dynamic analysis and design systems (DADS) [32]. To accurately model the ground reaction force between the feet and the ground, we used the Young's modulus-coefficient of restitution element (see Appendix C). By using this simulator, we can simulate the dynamic robot motion, and analyze various factors such as the necessary joint torque, joint speed, and the ground reaction force.

The parameters of the biped robot (Fig. 1) were set according to Table I. The biped's walking was simulated on our dynamic simulator. The walking speed was 2.0 [km/h] with the step length of 0.5 m/step and the step period of 0.9 s/step, the similar human walking parameters.

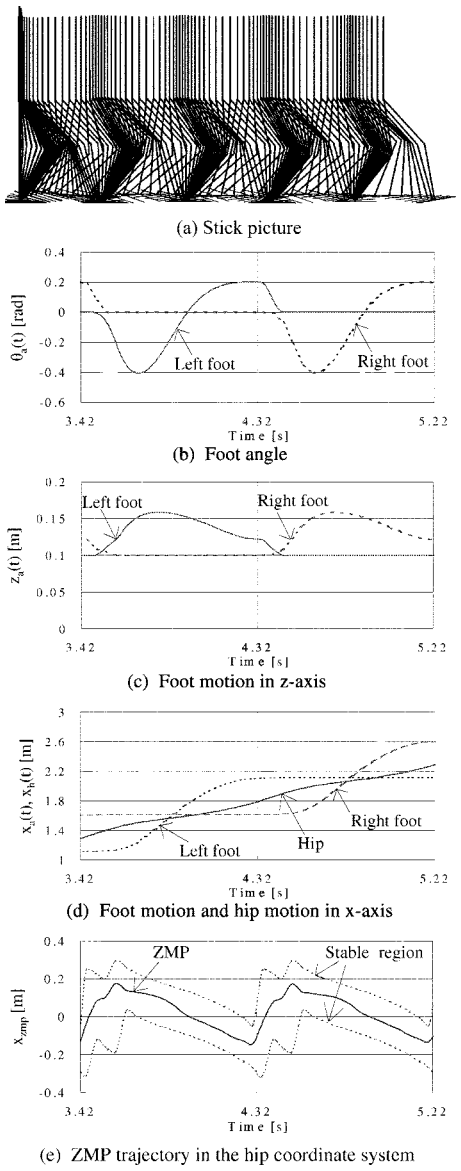

Fig. 5. Simulation results for level-ground walking, $q_{\mathrm{b}} = -0.2$ rad, $q_{\mathrm{f}} = -0.2$ rad, $L_{\mathrm{ao}} = 0.25$ m, $H_{\mathrm{ao}} = 0.16$ m.

A. Satisfaction of Stability and Ground Condition

Fig. 5 shows the simulation results for level-ground walking ($q_{\mathrm{gs}}(k) = 0$ rad, $q_{\mathrm{ge}}(k) = 0$ rad, $h_{\mathrm{gs}}(k) = 0$ m, $h_{\mathrm{ge}}(k) = 0$ m).

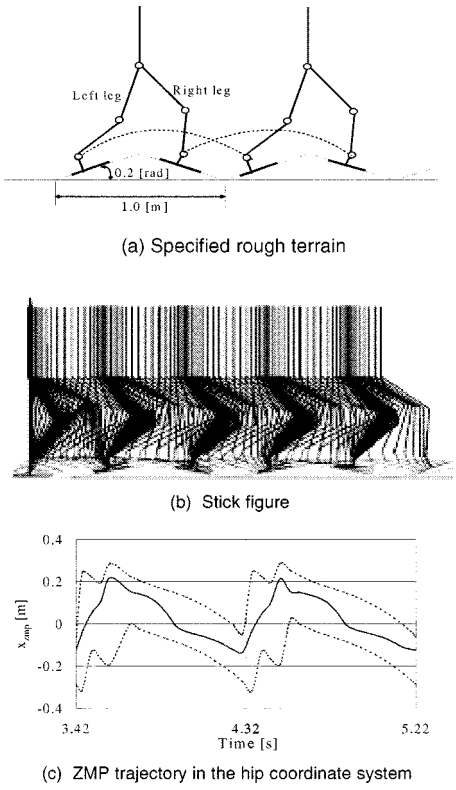

Fig. 6. Simulation results on rough terrain.

From the stick figure [Fig. 5(a)] and the foot angle [Fig. 5(b)], we can see both feet leave and land on the ground with the desired angles. Also, both foot trajectories [Fig. 5(b)–(d)] and the hip trajectory [Fig. 5(d)] are smooth, and the ZMP trajectory [Fig. 5(e)] is always near the center of the stable region, that is, the robot has a large stability margin.

Fig. 6 shows the specified rough terrain and the simulation results, respectively. In this simulation, the foot parameters were set as follows: $q_{\mathrm{gs}}(k) = 0.2$ rad, $q_{\mathrm{ge}}(k) = 0.2$ rad for the left foot, $q_{\mathrm{gs}}(k) = -0.2$ rad, $q_{\mathrm{ge}}(k) = -0.2$ rad for the right foot, and $q_{\mathrm{b}} = -0.2$ rad, $q_{\mathrm{f}} = 0.2$ rad, $L_{\mathrm{ao}} = 0.25$ m, $H_{\mathrm{ao}} = 0.08$ m for both feet. Both feet could match the ground slopes [Fig. 6(b)]. The ZMP in Fig. 5(e) is much more closer to the center of the stable region than the ZMP in Fig. 6(c). We can consider that this is because the walk on rough terrain is more complicated than the walk on level ground, and the robot needs to cost its stability for accomplishing complicated tasks.

$$
x_{\mathrm{h}}(t) = \begin{cases} kD_{\mathrm{s}} + \dfrac{D_{\mathrm{s}} - x_{\mathrm{ed}} - x_{\mathrm{sd}}}{T_{\mathrm{d}}^2(T_{\mathrm{c}} - T_{\mathrm{d}})}\big[(T_{\mathrm{d}} + kT_{\mathrm{c}} - t)^3 - (t - kT_{\mathrm{c}})^3 \\ \quad -T_{\mathrm{d}}^2(T_{\mathrm{d}} + kT_{\mathrm{c}} - t) + T_{\mathrm{d}}^2(t - kT_{\mathrm{c}})\big] + \dfrac{x_{\mathrm{ed}}}{T_{\mathrm{d}}}(T_{\mathrm{d}} + kT_{\mathrm{c}} - t) + \dfrac{D_{\mathrm{s}} - x_{\mathrm{sd}}}{T_{\mathrm{d}}}(t - kT_{\mathrm{c}}), & t \in (kT_{\mathrm{c}}, kT_{\mathrm{c}} + T_{\mathrm{d}}) \\ kD_{\mathrm{s}} + \dfrac{D_{\mathrm{s}} - x_{\mathrm{ed}} - x_{\mathrm{sd}}}{T_{\mathrm{d}}(T_{\mathrm{c}} - T_{\mathrm{d}})^2}\big[(t - kT_{\mathrm{c}} - T_{\mathrm{d}})^3 - (T_{\mathrm{c}} + kT_{\mathrm{c}} - t)^3 - (T_{\mathrm{c}} - T_{\mathrm{d}})^2(T_{\mathrm{c}} + kT_{\mathrm{c}} - t) \\ \quad -(T_{\mathrm{c}} - T_{\mathrm{d}})^2(t - kT_{\mathrm{c}} - T_{\mathrm{d}})\big] + \dfrac{D_{\mathrm{s}} - x_{\mathrm{sd}}}{T_{\mathrm{c}} - T_{\mathrm{d}}}(T_{\mathrm{c}} + kT_{\mathrm{c}} - t) + \dfrac{D_{\mathrm{s}} + x_{\mathrm{ed}}}{T_{\mathrm{c}} - T_{\mathrm{d}}}(t - kT_{\mathrm{c}} - T_{\mathrm{d}}), & t \in (kT_{\mathrm{c}} + T_{\mathrm{d}}, kT_{\mathrm{c}} + T_{\mathrm{c}}). \end{cases} \tag{10}
$$

As discussed above, a walking pattern that adapts to the ground conditions such as the roughness of the terrain and obstacles can be obtained by adjusting the values of $q_{\rm gs}(k)$, $q_{\rm ge}(k)$, $h_{\rm gs}(k)$, $h_{\rm ge}(k)$, $q_{\rm b}$, $q_{\rm f}$, $H_{\rm ao}$, and $L_{\rm ao}$. When the ground conditions and the stability constraint are satisfied, it is also possible to select a walking pattern requiring small specifications of the joint actuators discussed as follows.

B. Actuator Specifications and Walking Patterns

Fig. 7 shows the specifications of the joint actuators for level-ground walking with different foot clearances $H_{\rm ao}$ but with the same other parameters. It is known that a high foot clearance requires large peak torque and velocity of almost all the joints. We can consider that this is because the higher the swing foot lifts, the larger the energy required to drive the joint is. Therefore, to minimize the specifications of the joint actuators or the energy consumption, it is desirable to have a biped robot walk without excessively lifting the swing foot.

The simulation results for different hip height $H_{\rm h\,max}$ and $H_{\rm h\,min}$ but with the same other parameters are shown in Fig. 8. The peak torque of the knee joint for a high hip position is less than at a low hip position [Fig. 8(b)], but the other specifications is almost similar. We can consider that this is because the robot needs to bend its knee joint more at a low hip position, so large knee joint torque is required to support the robot. Therefore, from the viewpoint of reducing the load on the knee joint, it is essential to keep the hip at a high position.

Fig. 9 shows the actuator specifications of the knee joint on level ground and for different foot angles $q_{\rm b}$. Large peak torque [Fig. 9(a)] for a level foot slope $(q_{\rm b} = 0$ rad$)$ and large peak velocity [Fig. 9(b)] for a large foot angle $(q_{\rm b} = -1.0$ rad$)$ are required, respectively. We can explain these actuator specifications of the knee joint as follows. When the rear foot leaves the ground as in $q_{\rm b} = 0.0$ rad, the hip cannot be held at a high position, so the robot needs to bend the knee joint of its front support foot more. Therefore, large knee joint torque is required. On the other hand, it is possible for the hip to be held at a high position when $q_{\rm b} = -1.0$ rad. But, in this case, since it is necessary to lift the heel of the rear foot to a sufficient height at the end of the double-support phase, the required velocity of the knee joint increases, and consequently the required power of the knee joint increases.

C. Experiment

To test the validation of our proposed method, we also developed a biped robot (Fig. 10). The robot has 12 DOF, the total weight is 83 [kg], and its parameters are the same parameters as those in the simulation (Table I).

The 12 AC servo motors for the 12 joints are centrally controlled through input/output boards (digital-to-analog, analog-to-digital, and counter) by a control computer (Pentium 200 MHz). The control computer system and all motor driver units are mounted on the biped's body. The OS is RT-Linux, the servo rate is 1.0 [kHz].

According to simulation results of Sections V-A and V-B, we can select walking patters that satisfy the ground conditions, the constraints of stability and actuators by specifying walking parameters. Fig. 11 is an example of walking experiment for level ground with parameters $H_{\rm a0} = 0.16$ m, $H_{\rm h\,max} = 0.83$ m, $H_{\rm h\,min} = 0.82$ m, $q_{\rm b} = -0.2$ rad, and $q_{\rm f} = 0.2$ rad. We can observe that the robot's feet land on the ground heel first [Fig. 11(c) and (f)], and leave the ground with the toe in final contact [Fig. 11(d) and (g)].

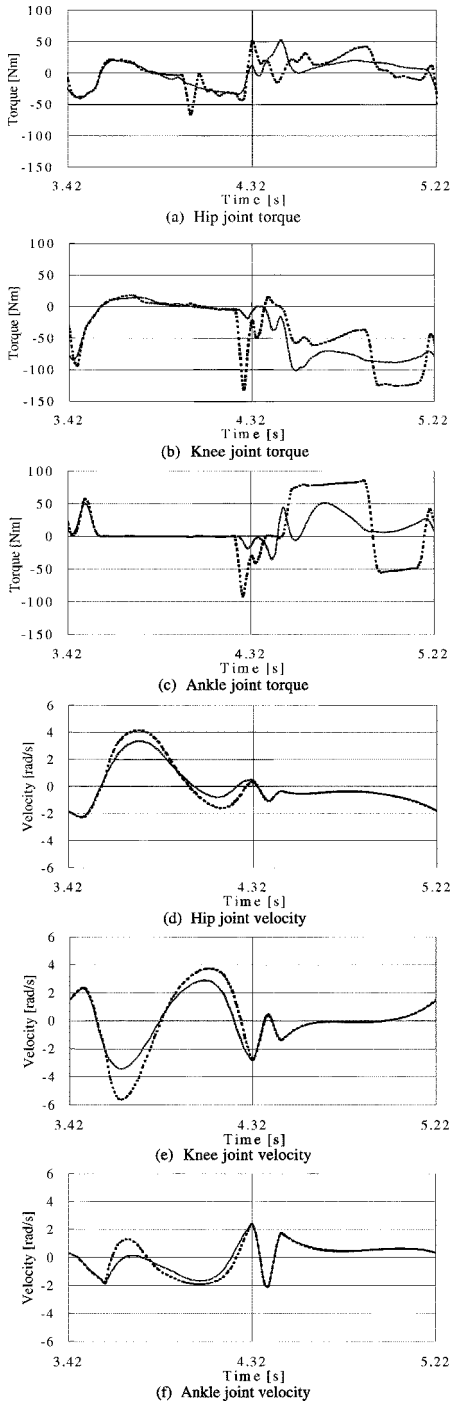

Fig. 7. Specifications for different foot clearances, $\cdots$: $H_{\rm ao} = 0.23$ m, —: $H_{\rm ao} = 0.16$ m.

VI. Conclusion

In this paper, we have described our proposed method for planning walking patterns for a biped robot. Our method has the following major contributions.

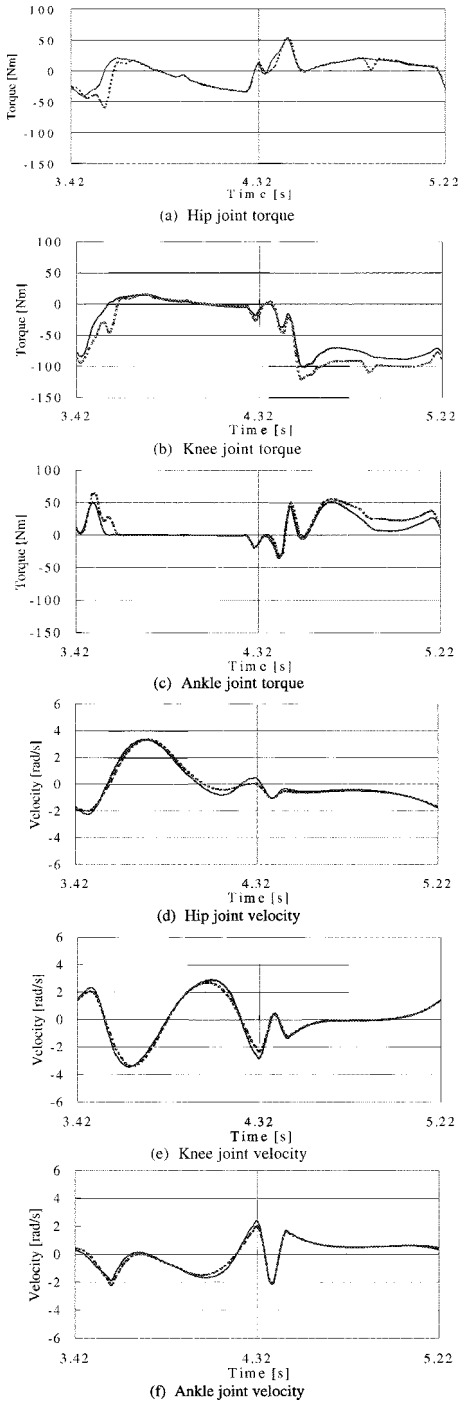

Fig. 8. Simulation results for different hip heights, $\cdots$: $H_{\mathrm{h}\max} = 0.80$ m, $H_{\mathrm{h}\min} = 0.79$ m; —:$H_{\mathrm{h}\max} = 0.83$ m, $H_{\mathrm{h}\max} = 0.83$ m.

1) The constraints including ground conditions and foot trajectory were formulated. Different foot motion can be produced by adjusting the values of the foot constraint parameters.
2) A method to formulate hip motion using only two parameters was proposed. This makes it possible to derive a highly stable, smooth hip motion without first designing the desired ZMP trajectory.
3) The correlation between the actuator specifications and walking patterns were clarified. Therefore, it is possible to select a walking pattern with small torque and velocity of the joint actuators after the ground conditions and the stability constraint are satisfied.
4) The proposed method was validated using a dynamic simulator and an actual biped robot.

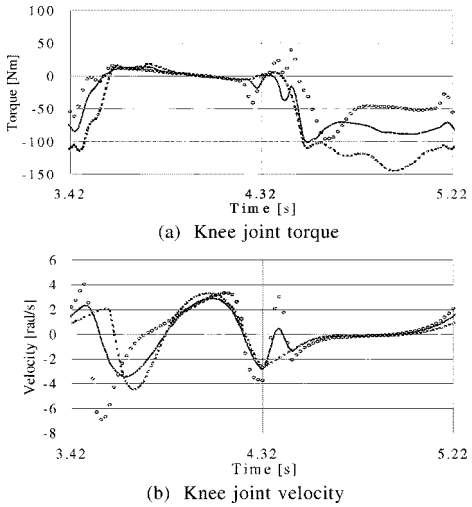

Fig. 9. Specifications for different foot slope, $\cdots$: $q_{\mathrm{h}} = 0.0$ rad, —: $q_{\mathrm{h}} = -0.2$ rad, ∘ ∘ ∘: $q_{\mathrm{h}} = -1.0$ rad.

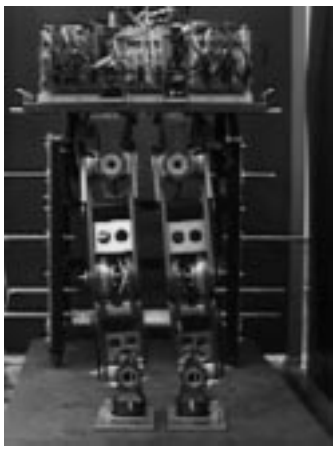

Fig. 10. Biped robot for experiment.

To deal with uncertainties in actual environments, real-time control based on sensor feedback is necessary. Our future study will focus on how to combine the planned walking pattern proposed in this paper and real-time control.

APPENDIX A
ZMP CRITERION

The ZMP can be computed using the following equations [28]:

$$x_{\mathrm{zmp}} = \frac{\sum_{i=1}^{n} m_i(\ddot{z}_i + g)x_i - \sum_{i=1}^{n} m_i\ddot{x}_i z_i - \sum_{i=1}^{n} I_{iy}\ddot{\Omega}_{iy}}{\sum_{i=1}^{n} m_i(\ddot{z}_i + g)} \tag{13}$$

$$y_{\mathrm{zmp}} = \frac{\sum_{i=1}^{n} m_i(\ddot{z}_i + g)y_i - \sum_{i=1}^{n} m_i\ddot{y}_i z_i - \sum_{i=1}^{n} I_{ix}\ddot{\Omega}_{ix}}{\sum_{i=1}^{n} m_i(\ddot{z}_i + g)} \tag{14}$$

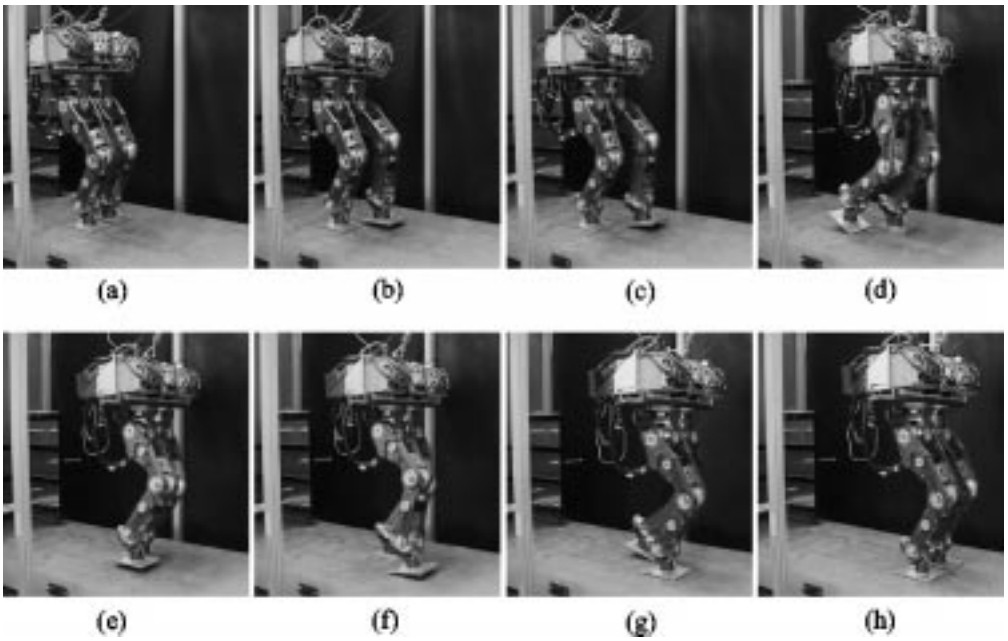

Fig. 11. Biped walking experiment.

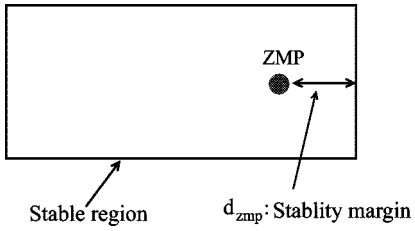

Fig. 12. Stable region and stability margin.

where m_i is the mass of link i (Fig. 1), I_{ix} and I_{iy} are the inertial components, $\ddot{\Omega}_{ix}$ and $\ddot{\Omega}_{iy}$ are the absolute angular velocity components around x-axis and y-axis at the center of gravity of link i, g is the gravitational acceleration, $(x_{\rm zmp}, y_{\rm zmp}, 0)$ is the coordinate of the ZMP, and (x_i, y_i, z_i) is the coordinate of the mass center of link i on an absolute Cartesian coordinate system.

If the ZMP is within the convex hull of all contact points (the stable region), the biped robot is able to walk. If the minimum distance between the ZMP and the boundary of the stable region is large, the moment preventing the biped robot from tipping over is large. The minimum distance $d_{\rm zmp}$ between the ZMP and the boundary of the stable region is called the stability margin (Fig. 12).

APPENDIX B
THIRD-ORDER SPLINE INTERPOLATION

For n breakpoints $t_1 < t_2 < \cdots < t_n$, $S(t_j) = f_j$, $j = 1, 2, \ldots, n$, the third-order spline function $S(t)$ is a third-order polynomial for each (t_j, t_{j+1}), and the first derivative $S'(t)$ and the second derivative $S''(t)$ are continuous on (t_1, t_n).

Letting $I_j = (t_j, t_{j+1})$, $h = t_{j+1} - t_j$, $S(t)$ is denoted by the following equation:

$$\begin{aligned} S(t) =& \frac{M_j}{6h_j}(t_{j+1} - t)^3 + \frac{M_{j+1}}{6h_j}(t - t_j)^3 \\ &+ \left(f_j - \frac{M_j h_j^2}{6}\frac{t_{j+1} - t}{h_j}\right) \\ &+ \left(f_{j+1} - \frac{M_{j+1}h_j^2}{6}\right)\frac{t - t_j}{h_j}. \end{aligned} \tag{15}$$

M_j is the solution of following equations:

$$\begin{cases} 2M_j + b_1 M_2 = d_1 \\ \dfrac{h_{j-1}}{6}M_{j-1} + \dfrac{h_j + h_{j-1}}{3}M_j + \dfrac{h_j}{6}M_{j+1} \\ \quad = \dfrac{f_{j+1} - f_j}{h_j} - \dfrac{f_j - f_{j-1}}{h_{j-1}}, \qquad j = 2, 3, \ldots, n-1 \\ a_n M_{n-1} + 2M_n = d_n \end{cases} \tag{16}$$

where

$$\begin{cases} a_j = \dfrac{h_{j-1}}{h_j + h_{j-1}} b_j = 1 - a_j, & j = 2, 3, \ldots, n-1 \\ c_j = \dfrac{f_{j+1} - f_j}{h_j}, & j = 2, 3, \ldots, n-1 \\ d_j = \dfrac{6(c_j - c_{j-1})}{h_j + h_{j-1}}, & j = 2, 3, \ldots, n-1. \end{cases} \tag{17}$$

When the initial constraint $S'(t_1) = 0$ and the end constraint $S'(t_n) = 0$, the following equations are obtained:

$$\begin{cases} b_1 = a_n = 1 \\ d_1 = \dfrac{6(f_2 - f_1)}{h_j} \\ d_n = -\dfrac{6(f_n - f_{n-1})}{h_{n-1}}. \end{cases} \tag{18}$$

$$F_n = \begin{cases} 0.733E_{\mathrm{m}}\sqrt{\frac{1}{r}}\left[1+\left(\frac{1-C_{\mathrm{r}}^2}{1+C_{\mathrm{r}}^2}\right)\tanh\left(2.5\frac{v_{\mathrm{p}}}{v_{\mathrm{r}}}\right)\right]\delta^{1.5}, & |v_{\mathrm{p}}| < |v_{\mathrm{t}}| \\ 0.733E_{\mathrm{m}}\sqrt{\frac{1}{r}}\left[1\pm 0.99\left(\frac{1-C_{\mathrm{r}}^2}{1+C_{\mathrm{r}}^2}\right)\right]\delta^{1.5}, & |v_{\mathrm{p}}| = \pm|v_{\mathrm{t}}| \\ 0.733E_{\mathrm{m}}\sqrt{\frac{1}{r}}\left[1+\left(\frac{1-C_{\mathrm{r}}^2}{1+C_{\mathrm{r}}^2}\right)\right]\delta^{1.5}, & |v_{\mathrm{p}}| > |v_{\mathrm{t}}| \end{cases} \tag{20}$$

APPENDIX C
YOUNG'S MODULUS-COEFFICIENT OF RESTITUTION

The spring-damper element is usually used to model the normal force between the feet and the ground as follows:

$$F_n = K_{\mathrm{f}}\delta + D_{\mathrm{f}}\dot{\delta} \tag{19}$$

where F_n is the ground normal force, δ is the penetration depth of the contact foot into the ground, K_{f} and D_{f} are the stiffness coefficient and the damping coefficient, respectively.

One main defect of the spring-damper element is the ground normal force may be negative, because $\dot{\delta}$ easily becomes negative just before the contact foot and the ground separate. A negative ground normal force implies that the ground pulls the contact foot, which is not correct physically in the case of usual ground.

In order to obtain a suitable model of the ground reaction force, the Young's modulus-coefficient of restitution element was used [37]. Let E_{m} be the Young's modulus of the contacting material, and C_{r} be the coefficient of restitution. If $C_{\mathrm{r}} = 0$, the contact is perfectly inelastic; if $C_{\mathrm{r}} = 1$, the contact is perfectly elastic. The ground normal force is given by (20), shown at the top of the page, where v_{p} and v_{t} denote the penetration velocity and the transition velocity between the contact foot and the ground, and r is the contact curvature. The friction force F_{f} is given by the following equation:

$$F_{\mathrm{f}} = \mu F_n \tag{21}$$

where μ is the nominal friction coefficient.

REFERENCES

[1] M. Vukobratovic and D. Juricic, "Contribution to the synthesis of biped gait," *IEEE Trans. Bio-Med. Eng.*, vol. BME-16, no. 1, pp. 1–6, 1969.

[2] F. Gubina, H. Hemami, and R. B. McGhee, "On the dynamic stability of biped locomotion," *IEEE Trans. Bio-Med. Eng.*, vol. BME-21, no. 2, pp. 102–108, 1974.

[3] I. Kato, S. Matsushita, T. Ishida, and K. Kume, "Development of artificial rubber muscles," in *Proc. Third Int. Symp. External Control of Human Extremities*, 1970, pp. 565–582.

[4] H. Miura and I. Shimoyama, "Dynamic walking of a biped," *Int. J. Robot. Res.*, vol. 3, no. 2, pp. 60–74, 1984.

[5] M. N Raibert, *Legged Robots That Balance*. Cambridge, MA: MIT Press, 1986.

[6] S. M. Song and K. J. Waldron, "An analytical approach for gait and its application on wave gaits," *Int. J. Robot. Res.*, vol. 6, no. 2, pp. 60–71, 1987.

[7] J. K. Hodgins and M. H. Raibert, "Adjusting step length for rough terrain locomotion," *IEEE Trans. Robot. Automat.*, vol. 7, pp. 289–298, June 1991.

[8] J. Fursho and M. Masubuchi, "A theoretically motivated reduced order model for the control of dynamic biped locomotion," *J. Dyn. Syst., Measure., Contr.*, vol. DSMC-109, pp. 155–163, 1987.

[9] S. Kajita, A. Kobayashi, and T. Yamamura, "Dynamic walking control of a biped robot along a potential energy conserving orbit," *IEEE Trans. Robot. Automat.*, vol. 8, pp. 431–438, Aug. 1992.

[10] W. T. Miller and A. L. Kun, "Dynamic balance of a biped walking robot," in *Neural Systems for Robotics*. New York: Academic, 1997, pp. 17–35.

[11] M. Garica, A. Chatterjee, and A. Ruina, "Speed, efficiency, and stability of small-slope 2-D passive dynamic bipedal walking," in *Proc. IEEE Int. Conf. Robotics and Automation*, 1998, pp. 2351–2356.

[12] J. H. Park and H. A. Chung, "Hybrid control for biped robots using impedance control and computed-torque control," in *Proc. IEEE Int. Conf. Robotics and Automation*, 1999, pp. 1365–1370.

[13] M. Y. Zarrugh and C. W. Radcliffe, "Computer generation of human gait kinematics," *J. Biomech.*, vol. 12, pp. 99–111, 1979.

[14] T. McGeer, "Passive walking with knees," in *Proc. IEEE Int. Conf. Robotics and Automation*, 1990, pp. 1640–1645.

[15] P. H. Channon, S. H. Hopkins, and D. T. Phan, "Derivation of optimal walking motions for a biped walking robot," *Robotica*, vol. 10, no. 2, pp. 165–172, 1992.

[16] M. Rostami and G. Bessonnet, "Impactless sagittal gait of a biped robot during the single support phase," in *Proc. IEEE Int. Conf. Robotics and Automation*, 1998, pp. 1385–1391.

[17] L. Roussel, C. Canudas-de-Wit, and A. Goswami, "Generation of energy optimal complete gait cycles for biped robots," in *Proc. IEEE Int. Conf. Robotics and Automation*, 1998, pp. 2036–2041.

[18] F. M. Silva and J. A. T. Machado, "Energy analysis during biped walking," in *Proc. IEEE Int. Conf. Robotics and Automation*, 1999, pp. 59–64.

[19] O. Bruneau, F. B. Ouezdou, and P. B. Wieber, "Dynamic transition simulation of a walking anthropomorphic robot," in *Proc. IEEE Int. Conf. Robotics and Automation*, 1998, pp. 1932–1397.

[20] Y. F. Zheng and J. Shen, "Gait synthesis for the SD-2 biped robot to climb sloping surface," *IEEE Trans. Robot. Automat.*, vol. 6, pp. 86–96, Feb. 1990.

[21] C. Chevallereau, A. Formal'sky, and B. Perrin, "Low energy cost reference trajectories for a biped robot," in *Proc. IEEE Int. Conf. Robotics and Automation*, 1998, pp. 1398–1404.

[22] A. Takanishi, M. Ishida, Y. Yamazaki, and I. Kato, "The realization of dynamic walking robot WL-10RD," in *Proc. Int. Conf. Advanced Robotics*, 1985, pp. 459–466.

[23] C. L. Shih, Y. Z. Li, S. Churng, T. T. Lee, and W. A. Cruver, "Trajectory synthesis and physical admissibility for a biped robot during the single-support phase," in *Proc. IEEE Int. Conf. Robotics and Automation*, 1990, pp. 1646–1652.

[24] K. Hirai, M. Hirose, Y. Haikawa, and T. Takenaka, "The development of honda humanoid robot," in *Proc. IEEE Int. Conf. Robotics and Automation*, 1998, pp. 1321–1326.

[25] A. Dasgupta and Y. Nakamura, "Making feasible walking motion of humanoid robots from human motion capture data," in *Proc. IEEE Int. Conf. Robotics and Automation*, 1999, pp. 1044–1049.

[26] D. W. Seward, A. Bradshaw, and F. Margrave, "The anatomy of a humanoid robot," *Robotica*, vol. 14, part 4, pp. 437–443, 1996.

[27] Q. Huang, S. Kajita, N. Koyachi, K. Kaneko, K. Yokoi, H. Arai, K. Komoriya, and K. Tanie, "A high stability, smooth walking pattern for a biped robots," in *Proc. IEEE Int. Conf. Robotics and Automation*, 1999, pp. 65–71.

[28] Q. Huang, S. Sugano, and K. Tanie, "Stability compensation of a mobile manipulator by manipulator motion: Feasibility and planning," *Adv. Robot.*, vol. 13, no. 1, pp. 25–40, 1999.

[29] C. Shih, "Gait synthesis for a biped robot," *Robotica*, vol. 15, pp. 599–607, 1997.

[30] ——, "Ascending and descending stairs for a biped robot," *IEEE Trans. Syst., Man., Cybern. A*, vol. 29, no. 3, 1999.

[31] Q. Huang, Y. Nakamura, H. Arai, and K. Tanie, "Development of a biped humanoid simulator," in *Proc. Int. Conf. Intelligent Robot and Systems*, 2000, pp. 1936–1942.
[32] E. J. Haug, *Computer-Aided Kinematics and Dynamics of Mechanical Systems, Basic Method*. Boston, MA: Allyn and Bacon, 1989.
[33] T. A. McMahon, *Muscles, Reflexes, and Locomotion*. Princeton, NJ: Princeton Univ. Press, 1984.
[34] V. T. Inman, H. J. Ralston, and F. Todd, *Human Walking*. Baltimore, MD: Willams & Wilkins, 1981.
[35] B. D. Bojanov, H. A. Hakopian, and A. A. Sahakian, *Spline Function and Multivariate Interpolation*. Norwell, MA: Kluwer, 1993.
[36] D. W. Marhefka and D. E. Orin, "Simulation of contact using a nonlinear damping model," in *Proc. IEEE Int. Conf. Robotics and Automation*, 1996, pp. 1662–1668.
[37] H. Han, T. Kim, and T. Park, "Tolerance analysis of a spur gear train," in *Proc. 3rd DADS Korean User's Conf.*, 1987, pp. 61–81.

Qiang Huang (M'98) was born in Hubei, China, in 1965. He received the B.S. and M.S. degrees in electrical engineering from Harbin Institute of Technology, Harbin, China, and the Ph.D. degree in mechanical engineering from Waseda University, Tokyo, Japan, in 1986, 1989, and 1996, respectively.

In 1996, he jointed the Mechanical Engineering Laboratory (MEL), Ministry of International Trade and Industry (AIST-MITI), Tsukuba, Japan, as a Research Fellow. He was a Researcher of Core Research for Evolutional Science and Technology (CREST) of the Japan Science and Technology Corporation (JST) at the University of Tokyo from 1999 to 2000. Currently, he is a Professor at the Department of Mechatronics, Beijing Institute of Technology, Beijing, China. His research interests include biped walking robots, humanoid and mobile manipulators.

Dr. Huang is a member of the IEEE Robotics and Automation Society.

Kazuhito Yokoi (M'91) was born in Nagoya, Japan, in 1961. He received the B.E. degree in mechanical engineering from the Nagoya Institute of Technology, and the M.E. and Ph.D. degrees in mechanical engineering science from the Tokyo Institute of Technology in 1984, 1986, and 1994, respectively.

In 1986, he joined the Mechanical Engineering Laboratory, AIST-MITI, Tsukuba, Japan, as a Researcher. He is currently a Senior Researcher of Humanoid Research Group, Intelligent Systems Institute, National Institute of Advanced Industrial Science and Technology (AIST), Tsukuba, Japan. From November 1994 to October 1995, he was a Visiting Scholar at the Robotics Laboratory, Computer Science Department, Stanford University. His research interests include humanoids, human-centered robotics, and mobile manipulator control.

Dr. Yokoi is a member of the IEEE Robotics and Automation Society and the IEEE Systems, Man, and Cybernetics Society.

Shuuji Kajita (M'91) received the master's degree in control engineering from the Tokyo Institute of Technology and the Dr.E. degree in control engineering from the Tokyo Institute of Technology, in 1985 and 1996, respectively.

In 1985, he joined the Mechanical Engineering Laboratory, Agency of Industrial Science and Technology, Ministry of International Trade and Industry (AIST-MITI). Meanwhile, from 1996 to 1997, he was a Visiting Researcher at the California Institute of Technology. Currently, he is a Senior Researcher at the National Institute of Advanced Industrial Science and Technology, Tsukuba, Japan, which was reorganized from AIST-MITI in April 2001. His research interests include robotics and control theory.

Kenji Kaneko received the B.E., M.E., and Ph.D. degrees in electrical engineering from KEIO University in 1988, 1990, and 1997, respectively.

In 1990, he joined the Mechanical Engineering Laboratory, AIST-MITI, Tsukuba, Japan, as a Researcher. He is currently the Senior Researcher of the Humanoid Research Group, Intelligent Systems Institute, AIST. His research interests include humanoid system integration, motion control, and macro–micro teleoperation.

Hirohiko Arai (M'91) received the B.E. and Ph.D. degrees in measurement and control engineering from the University of Tokyo, Tokyo, Japan, in 1982 and 1993, respectively.

From 1982 to 1984, he was with Honda Engineering Company, Saitama, Japan. He joined the Mechanical Engineering Laboratory, Agency of Industrial Science and Technology, Ministry of International Trade and Industry (AIST-MITI), Tsukuba, Japan, in 1984. He is currently the Chief of Skill and Dynamics Research Group, Intelligent Systems Institute, National Institute of Advanced Industrial Science and Technology, Tsukuba, Japan, which was reorganized from AIST-MITI in April 2001. His research interests include dynamic control of manipulators, control of nonholonomic systems, and power assist systems.

Noriho Koyachi (M'89) received the B.S. degree in mechanical engineering from Kyoto University in 1979.

He joined the Mechanical Engineering Laboratory, Agency of Industrial Science and Technology, Ministry of International Trade and Industry (AIST-MITI), in 1979. He is currently the Chief of Field Robotics Research Group, Intelligent Systems Institute, National Institute of Advanced Industrial Science and Technology (AIST), An Independent Administrative Institution (IAI) under the Ministry of Economy, Trade and Industry (METI), Tsukuba, Japan, which was reorganized from AIST-MITI in April 2001. His research interests include multilegged robot, legged mobile manipulator, and its applications.

Kazuo Tanie (M'85) was born in Yokohama, Japan, in 1946. He received the B.E., M.S. and Dr. Eng. degrees in mechanical engineering from Waseda University, Japan, in 1969, 1971, and 1980, respectively.

In 1971, he joined the Mechanical Engineering Laboratory (MEL), AIST-MITI, and served as the Director of Department of Robotics from April 1998 to March 2001. Since April 1, 2001, he has been with The National Institute of Advanced Industrial Science and Technology (AIST), which is an Independent Administrative Institution under the Ministry of Economy, Trade and Industry (METI), newly established based on the reorganization of the 15 research institutes under the former Agency of Industrial Science and Technology (AIST) in the Ministry of International Trade and Industry (MITI). Currently, he is the Director of Intelligent Systems Institute, AIST. Also, since 1992, he has been an Adjunctive Professor at the Graduate School of Systems and Information Engineering, University of Tsukuba, Japan, and since 1996, a Visiting Professor at the Advanced Research Center for Science and Engineering, Waseda University, Japan. From August in 1981 to August 1982, he was a Visiting Scholar at the University of California at Los Angeles, and in September 1995, he was a Visiting Professor at Scuola Superiore, Santa Anna, Italy. He has published more than 300 refereed papers in several domestic and international academic journals and the proceedings of international conferences. His research interests include sensory control of robotic arm and hand, virtual reality and its application to telerobotics, human skill understanding and its realization by nonlinear control, human friendly robot and humanoid.